—특별 강연—

Epitaxial Growth of Nickel Silicide ($NiSi_2$) in Vacuum Deposited Nickel and Gold Films on (III) Silicon Single Crystals*

Ki-Hyun Yoon** and Hee-Soo Lee***

규소(111) 단 결정에 진공 증착한 닉켈과 금 박막에서 $NiSi_2$의 적층성장

윤 기 현**·이 희 수***

순수한 닉켈과 금 박막을 (III)규소 단 결정위에 진공 증착시켰다. Ni/Au/Si 나 Au/Ni/Si 시료를 진공중에서 약 550°C로 가열하였을 때 육방정 혹은 변형된 육방정의 미소 결정들이 규소 기질위에 형성되었다. 이들 미소 결정들의 형성과정 및 조성은 X-선 회절법, scanning electron microscopy 및 scanning Auger microprobe 법을 사용하여 결정하였다. 이들 미소 결정은 $NiSi_2$임이 확인되었다.

Ni/Au/Si 시료에서는 Au-Si 공융점(370°C) 이상으로 온도가 증가됨에 따라 닉켈과 규소가 Au-Si 공융체 속으로 이동한후 반응하여 $NiSi_2$를 형성하였다.

Au/Ni/Si 시료에 있어서의 Au-Si 공융체 형성은 닉켈 박막에 있는 바늘구멍형의 표면 결함과 관련 지을수 있겠다. 금이 닉켈 박막의 grain boundary를 통하여 Ni/Si 계면으로 확산되어 그 계면을 습윤시킨 다음 Au-Si 공융체를 형성하였다.

이런 Au-Si 공융체는 닉켈과 규소 원자에 대한 높은 확산 매질로서 작용하여 $NiSi_2$ 형성을 촉진시켰다. 표면에 평행한 (III)규소면 위의 $NiSi_2$ 미소 결정은 유사한 육방정으로 나타났으며, 경사진 미소결정은 부등변 사변형과 유사하였다. Auger 스펙트럼및 Ni, Au 및 Si에 대한 내층조성 (in-depth Composition Profiles)은 $NiSi_2$ 미소 결정이 Au-Si 공융체의 matrix에 미소 부분으로 나타났음을 보여주었다.

INTRODUCTION

Increasing demands for large scale integrated circuits (LSI) have made imperative the development of practical and reliable multilevel metallization.

It has been reported[1] that the growth of a compound by reaction between a thin metal film and a single crystal can be controlled by processes at the substrate-metal interface, the compound-metal interface, or by transport of mate-

*1976년 춘계총회 특별강연
**Hongneung Machine Industry Co., LTD.
***Department of Ceramic Engineering, Yonsei University

rials through the reaction product layer.

In industrial applications, metal silicides on silicon are conventionally used to form ohmic contacts and Shottky barriers.[2] Silicides can be advantageous because they form at temperatures compatible with silicon device fabrication. Once formed, they should remain stable.

The purpose of this work was to identify, and determine the composition and the formation mechanism of the crystallites formed when silicon samples coated with nickel and gold films were heated to about 550°C. This temperature is far below the peritectic temperature (993°C) of the Si-richest nickel silicide.[3] This lowered reaction temperature has been associated with enhanced interdiffusion at the interface between the films.[4]

EXPERIMENTAL

Pure gold wire and nickel strip were separately evaporated from a resistively- heated U-shaped tungsten filament onto the unpolished (III) surface of n-type silicon wafers. The silicon subctrates were P doped with resistivities of 50 ohm cm. Ni/Au/Si samples were prepared by depositing gold on silicon substrates and then nickel upon the gold film. Au/Si and Au/Ni/Si samples were prepared in a similar fashion. Immediately before loading into the vacuum bell-jar for for metal deposition, the silicon substrates were rinsed in cold distilled water, degreased in acetone and etched in a dilute hydrogen fluoride solution for 1 minute to reduce the oxide thickness on the silicon substrates. The background pressure during evaporation was kept below 2×10^{-5} torr. The substrate-to-source distance was approximately 5 cm. During deposition, the temperature of the silicon substrates never exceeded about 50°C. The substrate temperature was determined by a chromel-alumel thermocouple held against to the substrate.

Immediately after evaporation, the adherence of the gold and nickel films to the silicon substrates was tested using the tape test[5,6]. In some cases, the films showed poor adherence and these samples were not used for further experiments. The ticknesses of the nickel and gold films were about 1100Å and 2800Å, respectively, as determined from Auger in-depth profiles.

The scanning electron microscope* (SEM) micrograph displayed in Fig. 1 shows that the silicon substrates were not smooth. Therefore, it is not surprising that these substrates were not smoothly covered by the deposited films.

Figure 1. SEM photograph of the microstructure of the surface of the unheated Si wafer. The Si substrate appears rough.

Many pinhole type defects appeared as dark spots on the surface of an untreated Au/Ni/Si sample.

The samples were heated in vacuum to about 550°C for approximately ten minutes by electron bombardment. The background pressure during heating the samples was maintained be-

*Model JSM-2. Japan Electronic Optic Laboratory Company, Japan

low 4×10^{-7} torr. After heating, the samples cooled to room temperature within a few minutes.

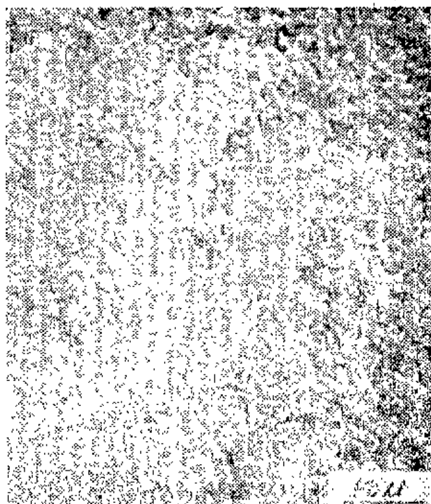

Figure 2. SEM photograph of the microstructure associated with the Au-Si eutectic in the Au/Si sample.

Figure 3. SEM photograph of the crystallites in the Ni/Au/Si sample. The crystallites are $NiSi_2$

The samples were then removed from the vacuum chamber and examined with a SEM. The surfaces of the samples showed microstruc-

Figure 4. SEM photograph of the crystallites in the Au/Ni/Si sample. The crystallites are $NiSi_2$

Figure 5. SEM photograph of the microstructure associated with Au-Si eutectic in the Au/Ni/Si sample. Au (light area) was recrystallized from the liquid Au-Si eutectic.

ture similar to the Au-Si eutectic structure found by Hellawell[7] and Sinha[8] in bulk gold-silicon alloys. Figure 2 shows the type of microstructure found for all samples. The microstructure in this figure was produced on a gold coated Si wafer.

Ni/Au/Si and Au/Ni/Si samples had other

features after heating. These features had the form of crystallites, as shown in Figs. 3 and 4. The shape of the crystallites resembles a slightly deformed hexagon. This shape is seen more clearly in Fig. 5.

Several analytical methods were employed to determine the composition of these crystallites and the matrix surrounding them. These methods were: X-ray diffraction; in-depth Auger electron spectroscopy; and SEM nondispersive X-ray analysis

A. X-Ray Diffraction Analysis

The crystallites formed on some samples were separated from the substrates by aqua regia. These crystallites were washed several times with distilled water to remove the residual gold solution. They were then dried in air, and examined by X-ray diffraction. Cerac* $NiSi_2$ powder was used for comparison with the crystallites.

Debye- Scherrer powder patterns were obtained using CuK_{α} radiation and a Ni filter. Some of the many lines on the sample pattern could be attributed to diffraction by pure gold. The diffraction lines of gold decreased in intensity with increased washing time. No shift in the positions of the gold lines occurred as a result of this treatment. This suggests that gold was not involved as a part of the crystallites. Auger electron analysis later confirmed this. The remainder of the sample lines were indexed as $NiSi_2$ which has a cubic calcium fluoride (Cl) structure[3, 9~11]. Table I lists the observed diffraction lines together with the calculated relative integrated intensities. The calculated lines for $NiSi_2$ could be accounted for except those lines whose intensities were so low as not to be visible on the X-ray film even after prolonged exposure.

TABLE II. Comparison of the Calculated Relative Integrated Intensities and Observed Intensities for $NiSi_2$ (a=5.406Å, CaF_2(Cl) Structure)

hkl	θ	d(Å) Calculated	I	I/I_1	d(Å) "Cerac"$NiSi_2$	d(Å) Observed	Observed Intensity
111	14.317	3.115	1928479	80	3.118	3.119	S
200	16.557	2.703	8064	<1	*	*	*
220	23.766	1.911	2420449	100	1.913	1.916	S
311	28.203	1.630	738672	31	1.631	1.632	W
222	29.575	1.561	372	<1	*	*	*
400	34.745	1.351	345438	14	1.352	1.354	VW
331	38.393	1.240	282595	12	1.241	1.243	VW
420	39.583	1.209	136	<1	*	*	*
422	44.268	1.103	720499	30	1.105	1.105	W
511	47.760	1.040	179627	7	1.042	1.045	VW
440	53.706	0.9557	315609	13	0.9559	0.9600	VW
531	57.450	0.9138	340110	14	0.9140	0.9143	VW
600	58.747	0.9010	184	<1	*	*	*
620	64.307	0.8547	728639	30	0.8548	0.8550	VW
533	69.117	0.8244	203402	8	0.8247	0.8250	VW

* not observed

It should be noted that $NiSi_2$ with a lattice parameter of 5.406Å represents a good match with the diamond structure[11] of Si with a lattice parameter of 5.4301 Å.

*Cerac/Pure Inc., Menomonee Falls, Wisconsin, U.S.A.

B. Auger Electron Analysis

An Auger spectrum from Ni/Au/Si sample before either heat treatment or sputtering is shown in Fig. 6. This spectrum was taken with a Scanning Auger Microprobe.*. Elemental oxygen and carbon peaks appear strongly at 513 and 273 eV, respectively. The nickel (MNN) peak at 60eV, and other nickel peaks with characteristic energies from 716 to 847 eV are prominent. Several gold peaks (70, 151, 1832–2111 eV) are observed. No silicon peaks are observed because the silicon substrate is too far (~2800Å) from the sample surface.

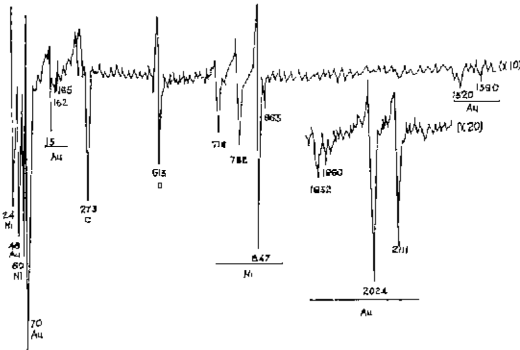

Figure 6. Auger spectra dN(E)/dE of the surface of an unheated Ni/Au/Si sample. (The numbers are expressed in eV).

The surface of the sample was not uniform because, as shown in Fig. 1, the silicon substrate itself has a rough surface. There were many pinholes in the nickel film. Gold was easily detected through these pinholes.

An Auger spectrum from the surface matrix of a Ni/Au/Si sample heated to about 550°C is shown in Fig. 7. The nickel peaks are no longer observed because the nickel had diffused into the gold layer. The silicon peaks are now

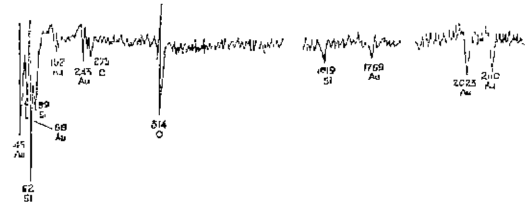

Figure 7. Auger spectra dN(E)/dE of the surface matrix of a Ni/Au/Si sample heated to 550°C (The numbers are expressed in eV).

at 82, 89, and 1619 eV. The peaks at 82 and 89 eV can be ascribed to the formation of oxidized silicon[12~14] at the surface rather than to an alloy formation of gold and silicon. The oxide was formed from exposure during transfer to the Auger spectrometer bell jar.

Figure 8 shows an in-depth composition profile[15] for the same surface matrix as Fig. 7. The nickel intensity is very weak over the entire depth. The gold intensity is very strong to about 1500Å. This region may be a Au-Si alloy. Beyond 1500Å, the silicon intensity is increased since this marks the beginning of the silicon substrate.

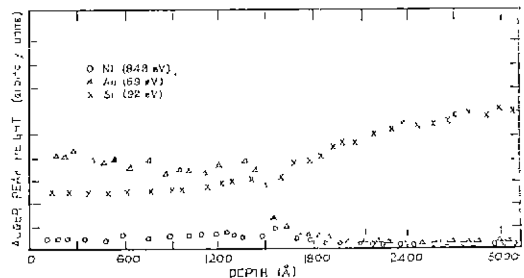

Figure 8. In-depth composition profile for Ni, Au, and Si of the surface matrix of a Ni/Au/Si sample heated to 550°C for 10min.

Figure 9 shows an Auger spectrum taken from a crystallite of the type shown in Fig. 5. The silicon peak (LVV) is represented by two peaks at 86 and 92 eV. The gold peak (MNN)

*Physical Electronics Industries, Eden Prairie, Minnesota, U. S. A.

appears at 71 eV which is the same position as in Fig. 7. The gold peak (MNN) intensity is greatly reduced compared with that of the nickel peak (MNN) at 62 eV. According to Hass et al.[16], since there is no difference of electronegativity between silicon and nickel, the silicon Auger peak at 92 is not expected to shift.

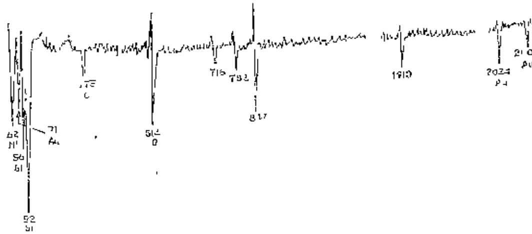

Figure 9. Auger spectra dN(E)/dE of the crystallites of a Ni/Au/Si sample heated to 550°C (The numbers are expressed in eV).

Figure 10 shows an in-depth composition profile of a crystallite from the heated Ni/Au/Si sample. Strong and almost uniform nickel and silicon intensities are observed until a depth of about 5100Å. The increase in silicon and nickel peak intensities was probably due to the decrease of carbon and oxygen surface contamination with depth. This region ceems to be mainly $NiSi_2$. Beyond 5100Å, the silicon intensity is very great since this marks the beginning of the silicon substrate. Here, the nickel intensity decreases rapidly.

C. Non-Dispersive X-ray Analysis

The Auger electron spectra, as well as the Auger in-depth composition profiles of crystallites on the silicon substrates, showed that these crystallites contained gold to a depth of over 1000Å. Therefore, in order to study the gold-free region with non-dispersive X-ray analysis, the gold containing layer was removed by ion sputtering. The sputter-etched crystallites were then examined in SEM. An Ortec non-dispersive X-ray unit was used to obtain a chemical analysis of the crystallites. Since X-ray diffraction of the separated crystallites had shown them to be $NiSi_2$, a sample of Cerac* $NiSi_2$ was used in the SEM unit for comparison purposes. Separated crystallites were also examined in the SEM unit.

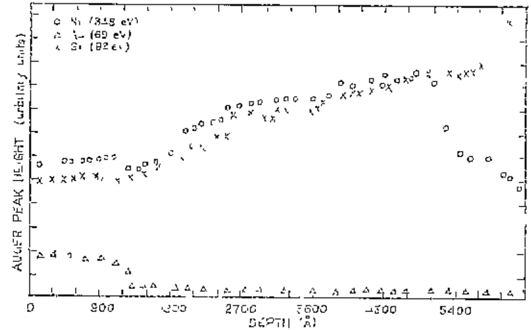

Figure 10. In-depth composition profile for Ni, Au and Si of the crystallites of a Ni/Au/Si sample heated to 550°C for 10min.

TABLE II List of Peaks Height and Intensity Ratio of Si and Ni in the Crystallites on the Surface of the Sample, the Crystallites Separated from the Sample and Cerac* $NiSi_2$ Taken by the SEM X-ray Analyzer.

Sample	Si Peak	Ni Height (cm)	Si/Ni Intensity Ratio
Crystallites on the Sample	3.2	1.6	2
Crystallites Seperated from the Sample	1.0	0.5	2
Cerac $NiSi_2$	4.0	2.0	2

* Cerac/Pure, Inc., Menomonee Falls, Wisconsin, U. S. A.

The peak heights, which are proportional to the number of X-ray puleses, recorded by the Ortec non-dispersive X-ray unit, are shown in Table II. For all samples examined, the ratio of the silicon and nickel X-ray counts is two

*Cerac/Pure Inc., Menomonee Falls, Wisconsin, U. S. A.

to one. For the crystallites alone, this fact does not prove that their composition is $NiSi_2$, since the instrument may not have the same sensitivity for each element. However, the fact that the same ratio is obtained for a sample of known composition does support the conclusion that the crystallites are indeed composed of $NiSi_2$.

D. Mechanism of the Formation of $NiSi_2$

In the Ni/Au/Si sample, it is likely that the gold film reacted with the silicon substrate as the temperature increased over the Au-Si eutectic temperature (370°C). Both nickel and silicon atoms could easily migrate into the eutectic and react to form $NiSi_2$.[17] In the Au/Ni/Si sample, it is probable that gold diffused through pinhole type defects and grain boundaries of the nickel film to the Ni/Si interface. The gold and silicon then reacted to form the Au-Si eutectic. This liquid eutectic probably acted again as a high difiusivity medium for nickel and silicon atoms which then reacted to form $NiSi_2$. In both cases, gold might have been separated from the Au-Si eutectic when the silicon in the eutectic reacted with nickel and some of the Au-Si eutectic might have remained on the surface.

The unit cells of both Si and $NiSi_2$ contain eight silicon atoms so that only a short range movement of the silicon atoms would be requi-red for precipitation of the long range diffusing interstitial nickel atoms. From the similarity of

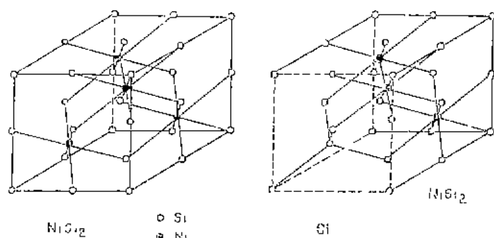

Figure 11. Schematic representation of the $NiSi_2$ and the Si-$NiSi_2$ interface.

structures and lattice parameters of both Si and $NiSi_2$, expitaxial growth of the $NiSi_2$ on the silicon substrate can be expected. If the two structures are matched along a (III) plane as illustrated in Fig. 11, it can be seen that the atomic arrangements are matched and form a coherent interface. It has been observed[18] that the bulk precipitates lie in lines in the crystal. This has been suggested as being due to hete-rogeneous nucleation by dislocations, providing vacancies for the precipitation. The precipita-tion of $NiSi_2$ does not require a steady vacancy source the unit cells of both Si and $NiSi_2$ con-tain the same number of silicon atoms. Indeed, it seems that the hexagonal crystallites lie with their (III) plane parallel to the (III) silicon substrate surface. The $NiSi_2$ crystallites which lie on the (III) substrate plane parallel to the surface appear as regular hexagons, while the inclined crystallites resemble trapezia.

CONCLUSION

$NiSi_2$ crystallites are formed when Ni/Au/Si and Au/Ni/Si thin film samples are heated to 550°. They appear to be formed by the rapid diffusion of Ni and Si in an Au-Si eutectic which forms at the Si surface. The orientation of the crystallites indicates they grow epitaxi-ally at the (III) silicon surface. The nickel originally present as a thin film is incorporated into the crystallites. After formation, the crys-tallites are surrounded by an Au-Si matrix. Evidently, in the presence of a gold-silicon eut-ectic, $NiSi_2$ crystals can grow at temperatures much lower than 993°C.

REFERENCES

1. M. P. Lepselter and J. M. Andrews, *Ohmic Conta-cts to Semiconductor* (ed. by B. Schwartz), *Electrochem. Soc.*, (1969).
2. J. F. Ziegler, J. W. Mayer, C. J. Kircher and

K. N. Tu, *J. Appl. Phys.*, **44**, 3851(1973).
3. M. Hansen, *Constitution of Binary Alloys*, McGraw-Hill Book Co., Inc., New York (1958).
4. G. Ottaviani, D. Sigurd, V. Marrello, J. W. Mayer and J. O. McCaldin, *J. Appl. Phys.*, **45**, 1930(1974).
5. J. Strong, *Rev. Sci. Instrum.*, **6**, 97(1935).
6. L. Holland, *Vacuum Deposition on Thin Films*. John Wiley and Sons, Inc., New York (1956).
7. A. Hellawell, *Prog. Mater. Sci.*, **15**, 1(1970)
8. A. K. Shina, *Thin Solid Films*, **20**, 115(1974)
9. J. W. Mayer and K. N. Tu. *J. Vac. Sci. Technol.*, **11**, 86(1974).
10. C. Picker and P. S. Dobson, *Crystal Lattice Defects*, **3**, 219(1972).
11. A. C. Wilson(ed.) *Structure Reports*, Vol. 13, N. V. A. Oostnoek's Uitgevers MIJ Utrecht (1954).
12. C. C. Chang, *Surf. Sci.*, **25**, 53(1971).
13. S. Thomas, *J. Appl. Phys.*, **45**, 161(1974).
14. G. W. Stupian, *J. Appl. Ppys.*, **45**, 5278(1974).
15. Each peak-to-peak deflection in the derivative of the energy distribution versus energy curve is called an Auger electron peak. While recording the peak-to-peak amplitudes of the Auger electron peaks, in-depth composition profiles were obtained by argon ion sputtering of the thin film.
16. T. W. Haas, J. T. Grant and G. J. Dooley III, *J. Appl. Phys.*, **43**, 1853 (1972)
17. K. H. Yoon, G. Lewis and L. L. Levenson, *J. Eletronic Materials*, **5**, 263(1976)
18. M. Yoshida, Y. Yamagochi and H. Aoki, Japan, *J. Appl. Phys.*, **2**, 305(1963).

[필자소개]

윤 기 현

연세대학교 화학과 및 대학원 졸업, 연세대학교 이공대학 전임강사, University of Missouri에서 박사과정 및 Postdoctoral Fellow. 현재 홍능기계공업사 근무, 공학박사.

이 희 수

연희전문 수물과, 서울공대 화공과 졸업, 인하대, 한양대 교수를 거쳐 현재 연세대 교수, 연세대 이공대 공학부장, 전 요업학회 회장, 공학박사.